Computers & Geosciences 35 (2009) 2111–2118

Contents lists available at ScienceDirect

Computers & Geosciences

journal homepage: www.elsevier.com/locate/cageo

Modelling and compact inversion of magnetic data: A Matlab code ☆

S. Stocco *, A. Godio, L. Sambuelli

DITAG, Politecnico di Torino, C.so Duca degli Abruzzi 24, 10129 Torino, Italy

ARTICLE INFO

Article history:
Received 15 January 2008
Received in revised form
8 April 2009
Accepted 15 April 2009

Keywords:
Magnetic prospection
Modelling and inversion
Model resolution

ABSTRACT

The modelling and inversion of the total magnetic field (TMF), its vertical gradient (VGTMF) and the vertical component of TMF (VMF) according to the basic principle to minimize the cross-sectional area of the source bodies are described. The software code, with an interactive graphical interface, operates in Matlab environment (version 7.0). The code of the inversion procedure is based on a weighted–damped least-squares algorithm, according to a criterion of balancing the weight of the data inaccuracies and the compactness of the solution. We have applied the approach to both synthetic and field data. This software can be used for didactical purposes or for a fast estimate of magnetic source bodies in archaeological and environmental prospecting.

1. Introduction

A magnetic survey is one of the most popular geophysical techniques for the fast mapping of large areas in archaeological and environmental prospecting. The survey consists of mapping one or more components of the earth's geomagnetic field in order to analyse the magnetic field anomalies. The interpretation of the magnetic anomalies involves pointing out the spatial location, the shape and the magnetic properties (magnetic susceptibility) of the source buried bodies. Among the many approaches and techniques available for quantitative interpretation, some of the most popular involve inversion processes that allow the best model of the susceptibility distribution in the subsoil to be determined, from an automatic- or semi-automatic analysis of the observed data. We have implemented a Matlab code that allows the total magnetic field (TMF), its vertical gradient (VGTMF) and the vertical component of TMF (VMF) to be modelled and inverted by minimizing the cross-sectional area of the source bodies. This principle is derived from the original approach by Last and Kubik (1983). The code is based on a forward model tool (2D and $2\frac{1}{2}$D) that considers the subsoil to be made up of 2D or $2\frac{1}{2}$D horizontal prisms orthogonal to the survey line/profile and the remanent magnetisation effect is also incorporated. A graphical interface allows the magnetic susceptibility to be assigned to each prism in the vertical section. The parameters for the forward analysis to be chosen are the inducing earth's magnetic field intensity, magnetic inclination, angle between the profile direction and the magnetic north. The code also incorporates an inversion tool that allows the parameters to be selected for the inversion procedure of the magnetic data: the number of iterations, the damping parameter and the expected susceptibility contrast of the target. Other statistical parameters are introduced to guide the best fit between the computed and observed data. A simple data filtering tool is implemented for a fast pre-processing of the data that has to be inverted. According to the basic principle of minimizing the volume of the source magnetic body, the method is suitable for application in engineering, environmental and archaeological fields. We present some synthetic examples in order to explore the effectiveness and the limits of the method.

The use of Matlab program codes for magnetic data processing is well documented. Cooper and Cowan (2006) compared the results of different filters on synthetic gravity data and on magnetic data from Australia using a Matlab code. Cooper (2006) showed the use of continuous wavelet transform in the analysis of magnetic or gravity data in order to obtain the location and depth estimates of gravity and magnetic sources. The use of continuous and discrete wavelet transform in potential field data is also well documented (Fedi and Quarta, 1998; Fedi et al., 2004; Moreau et al., 1997).

Automatic techniques, such as Euler deconvolution, have come into common use as an aid to interpret profile or gridded survey data (Durrheim and Cooper, 1998). This method provides an automatic estimate of source location and depth, introducing the concept of the structural index (SI) to characterise families of source types (e.g. FitzGerald et al., 2004).

A method for the inversion of vertical, horizontal or total magnetic field anomalies over thin sheets, thick dikes and vertical faults was described by Venkata Raju (2003). The initial solution is

Abbreviations: TMF, total magnetic field; VMF, vertical component of the TMF; VGTMF, vertical gradient of the TMF; EMF, earth's magnetic field; R.M., remanent magnetisation; N/S, noise-over-signal ratio

☆ Code available from server at http://www.iamg.org/CGEditor/index.htm.

* Corresponding author. Tel.: +39 011 0907737.
E-mail addresses: stefano.stocco@polito.it (S. Stocco), alberto.godio@polito.it (A. Godio), luigi.sambuelli@polito.it (L. Sambuelli).

0098-3004/$ - see front matter © 2009 Elsevier Ltd. All rights reserved.
doi:10.1016/j.cageo.2009.04.002

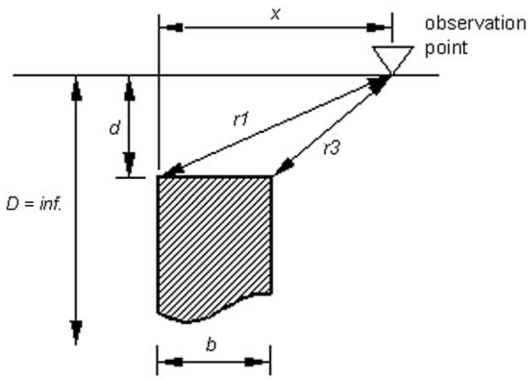

Fig. 1. Distances and angles for synthetic anomaly determination for a $2\frac{1}{2}$D vertical prism with infinite depth extent.

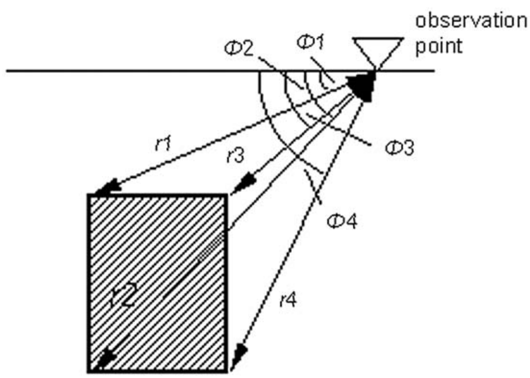

Fig. 2. Geometry of a vertical prism of finite depth extent.

modified in an iterative process using non-linear least-squares regression by employing Marquardt's algorithm implemented in FORTRAN 77. The regional value, which is subjective in manual interpretation, is also adjusted in this method to improve the fit between experimental and computed data.

Narasimha Rao et al. (1995) implemented a computer program called GMINV for inversion of potential field data using the damped approximate technique. The program runs in DOS or UNIX environment.

2. Materials and methods

The interpretation of magnetic data can sometimes involve two steps, calculation of the direct problem (forward modelling) and solution of the inverse problem (inversion). Forward modelling allows one to compute the theoretical response due to magnetic source bodies, assuming some hypothesis on the shape and the volume of the magnetic body and the susceptibility contrast between the body and the hosting environment. The analytical solutions to these problems are usually given for bodies of simple shape and regular geometry.

The inversion procedure considers the observed profiled or gridded data and, using an optimisation procedure, estimates the distribution of the susceptibility, shape and volume of the buried magnetic bodies. This step is usually affected by some ambiguities due to the ill-poseness of the problem, the ill-conditioning of the linear or linearized systems and the difficulties involved in governing the propagation of the uncertainties in the solution. The approach here considered, which minimizes the aforementioned shortcomings, has been introduced, widely discussed and refined by several authors (e.g. Last and Kubik, 1983; Guillen and Menichetti, 1984). The code can be used to model the magnetic

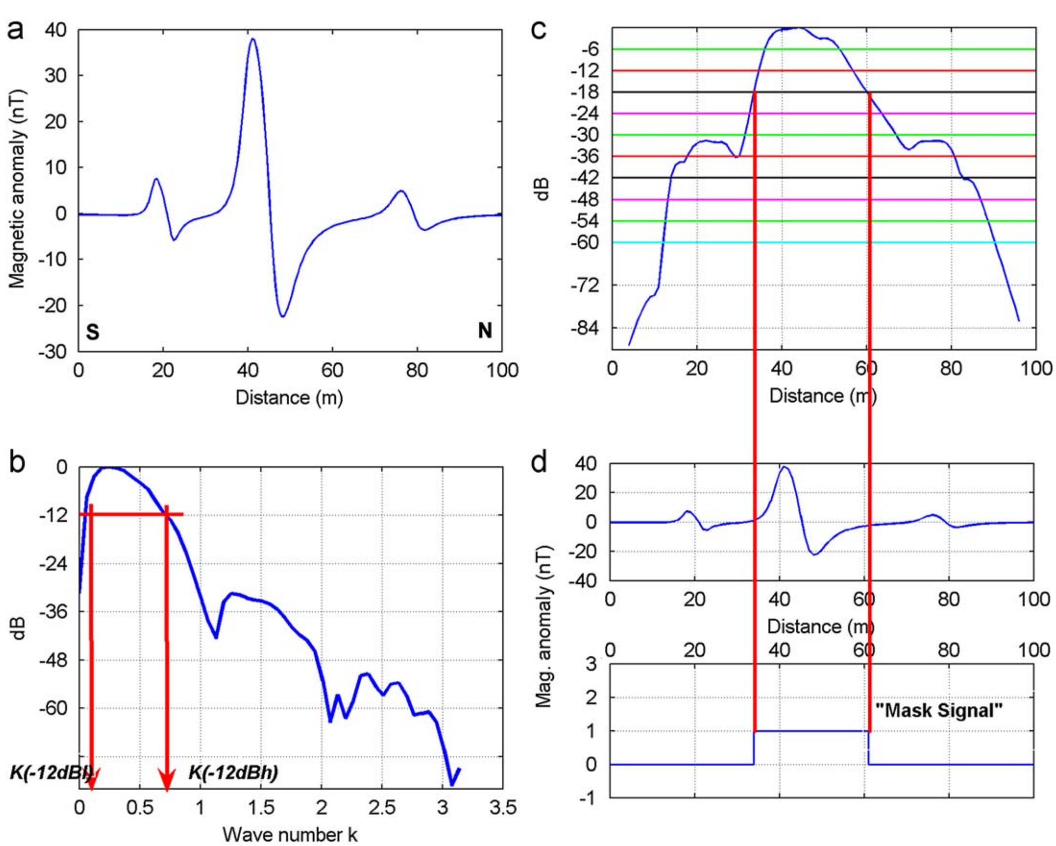

Fig. 3. Determination of "mask signal": (a) synthetic signal (profile direction is *S–N*), (b) spectrum, (c) signal running power and (d) "mask signal".

response of bodies with simple shapes and for a fast inversion thanks to the introduction of some improvements, with respect to the conventional approach that maximizes the compactness of the magnetic source bodies. It can be used on some selected magnetic profiles extracted from maps to estimate the size and depth of elongated source bodies. In the following, we highlight the presentation of the modelling procedure and the aspects on the inversion procedure.

2.1. Forward modelling

We implemented a 2D code to model TMF anomalies. A magnetic body can be defined to be 2D when its strike length in the direction perpendicular to the profile is at least 10 times its width (Telford et al., 1990, p. 94). We extended the field of application of the code to the $2\frac{1}{2}$D condition by introducing the possibility of giving a finite strike length to the bodies, even though the modelling is two dimensional; in such a case, we refer to a $2\frac{1}{2}$D model and its analytical solution is (Telford et al., 1990, p. 95)

$$F = kF_e G \tag{1}$$

with

$$\begin{aligned} G = {} & \sin^2 I \sin\beta [\ln\{(r_1^2+L^2)^{1/2}+L\} - \ln\{(r_1^2+L^2)^{1/2}-L\} \\ & + \ln\{(r_3^2+L^2)^{1/2}-L\} - \ln\{(r_3^2+L^2)^{1/2}+L\}] - (\cos^2 I \sin\beta - \sin^2 I) \\ & \times \left[\tan^{-1}\left(\frac{L}{x}\right) - \tan^{-1}\left(\frac{L}{x-b}\right) - \tan^{-1}\left\{\frac{Ld}{x(r_1^2+L^2)^{1/2}}\right\}\right. \\ & \left. +\tan^{-1}\left\{\frac{Ld}{(x-b)(r_3^2+L^2)^{1/2}}\right\}\right], \end{aligned} \tag{2}$$

where F is the total field; F_e the EMF intensity; k the susceptibility contrast between the magnetic target and the host medium; I the earth's magnetic field inclination; β the strike angle of the prism relative to the magnetic north; r_i, d, b are the geometric values of distances and angles (Fig. 1); L is the half-strike length of the prism; x the coordinate of the observation point.

Eq. (2) refers to a vertical prism with an infinite depth extent. The simplest way of dealing with the problem is to discretise the spatial domain into rectangular prisms with the hypothesis that the magnetic characteristic must be constant in each prism. It is possible to obtain the total magnetic field for each prism of finite vertical extent by evaluating Eq. (2) for both the top and the bottom of the prism itself and then subtracting the results

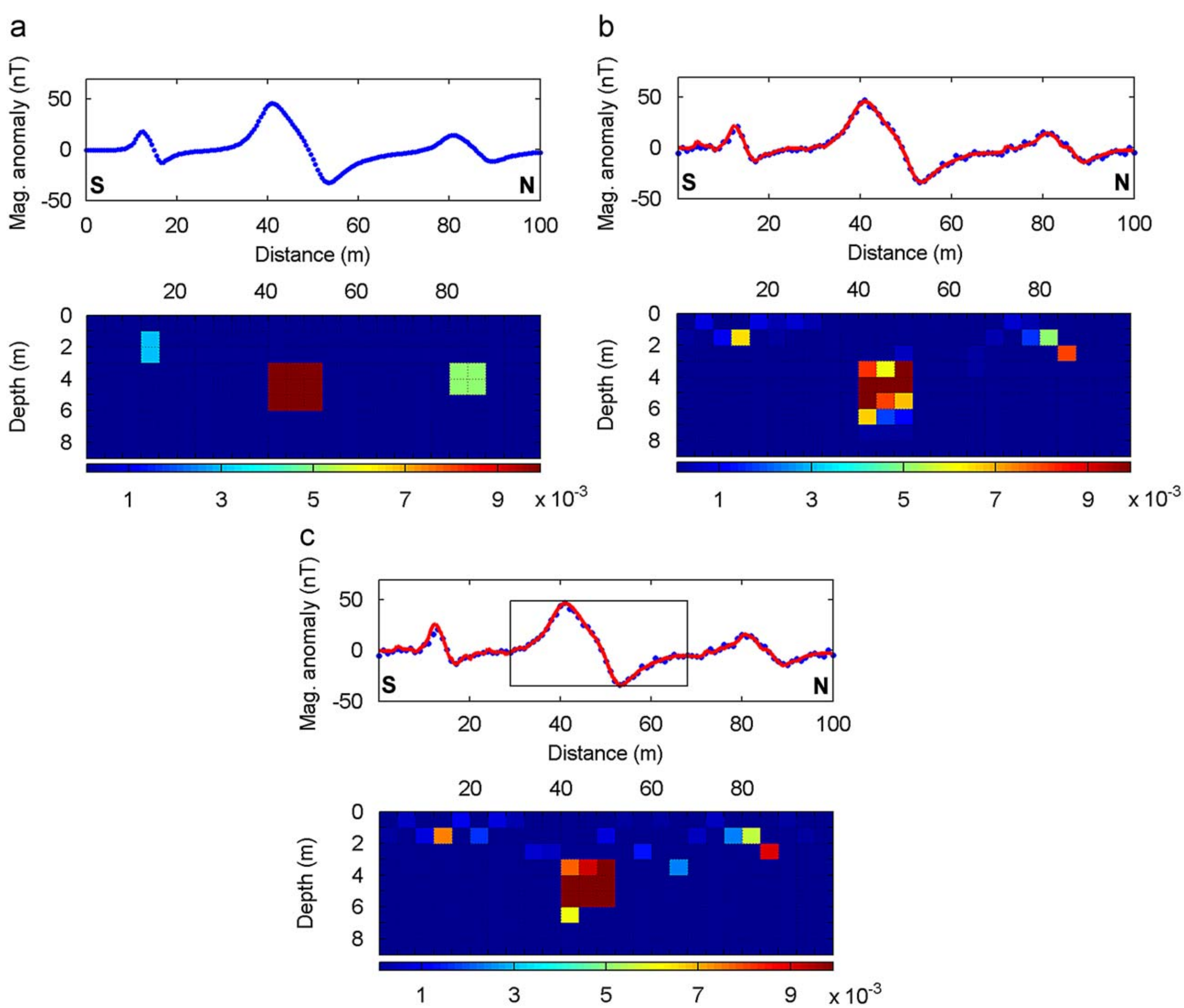

Fig. 4. Example of use of "mask signal": (a) synthetic model (profile direction is S–N), (b) inversion result without using "mask signal" and (c) using mask signal.

(Bhattacharyya, 1964). If the computation is performed for each prism at each measured point, the result is a kernel matrix with the same number of rows as measuring points and the same number of columns as discretisation prisms. Using the previously presented procedure, we evaluate the kernel associated to the VMF and VGTMF.

Eq. (1) evaluates the magnetic anomaly caused by a body with or without negligible remanent magnetisation (R.M.). In this case, the vector of the induced magnetisation is in the same direction as the vector of the EMF. The resultant vector is no longer parallel to the inducing field for a body characterised by an R.M. We added the possibility of assigning an R.M. to the body in the forward modelling and we evaluate the total magnetic anomaly of the resultant field.

The input parameters for R.M. are the Königsberger ratio (Q), defined as the ratio between the amplitude of the remanent and induced magnetisation; and the angles with respect to the horizontal (inclination—α_1) and to the magnetic North (declination—α_2).

With some magnetometers (for example flux-gate) only a component of the TMF can be measured, usually the VMF, so the possibility of modelling the response of the vertical component is also included. In this case the kernel G for a 2D prism is (Telford et al., 1990, p. 95)

$$G = 2\,[\cos I \,\sin \beta \,\ln(r_2 r_3/r_4 r_1) - \sin I\,(\Phi_1 - \Phi_2 - \Phi_3 + \Phi_4)], \tag{3}$$

where r_i and ϕ_i are distances and angles, as shown in Fig. 2.

The kernel matrix is computed using the same approach described for the $2\frac{1}{2}$D case.

We further implemented a rapid trial-and-error method: by using a graphic interface it is possible to change the values of the susceptibility contrast at each pixel in the spatial domain, compute the forward modelling, compare the evaluated data with the experimental ones, change the susceptibility contrast of other pixels, and so on, until an acceptable fitting between the synthetic and experimental data is obtained. The result can be used as a starting model in the inversion procedure.

2.2. Inversion

The principle of the compact inversion (Last and Kubik, 1983) involves minimizing the area (volume in 3D problems) of the source body, which is the same as maximizing its compactness.

As most of the cases, we deal with are slightly underdetermined problems, we need to solve the inversion problem using the weighted–damped least-squares method. The formulation is

$$v = W_v^{-1} G^T (G W_v^{-1} G^T + W_e^{-1})^{-1} d, \tag{4}$$

where having m prisms of unknown susceptibility and n measured data: v is the unknown susceptibility vector ($m \times 1$); d the observed magnetic data set ($n \times 1$); W_v the susceptibility weighting matrix ($m \times m$); W_e the noise-weighting matrix ($n \times n$); G the kernel ($n \times m$); W_v and W_e are diagonal matrices. The susceptibility weighting matrix has the form (Last and Kubik, 1983)

$$[W_v^{(k-1)}]_{ii}^{-1} = [v_i^{(k-1)}]^2 + \varepsilon, \tag{5}$$

where k is the iteration and ε the perturbation number whose value is between 10^{-13} and 10^{-10}.

The noise-weighting matrix is an *a posteriori* covariance matrix that depends on the susceptibility weighting matrix, the kernel, and a parameter that states the a priori estimated noise-to-signal ratio (N/S), as will later be explained. This matrix has the form

$$W_e^{-1} = (N/S)\, diag(G W_v^{-1} G^T). \tag{6}$$

The method consists of an iterative procedure in which the weighting matrices change at each iteration until a satisfying convergence of the solution is obtained (Last and Kubik, 1983).

We implemented in the code the possibility of dealing with: (1) TMF or VMF data of a single sensor; (2) VGTMF data; (3) a joint inversion of the TMFs or VMFs data of two sensors.

The input parameters for the inversion procedure are: (1) maximum number of iterations; (2) maximum allowed value of susceptibility contrast (minimum in case of negative susceptibility contrast between the source body and the background, as for cavities); (3) noise-over-signal ratio.

In order to assure the quality of the best fit and the reliability of the model parameters, the model resolution matrix and the singular value decomposition of the kernel are computed.

The model resolution matrix indicates whether the model parameters can be independently predicted or resolved (Menke, 1984, p. 64). By selecting a threshold in the model resolution matrix, it is possible to evaluate the best subsoil gridding and to determine the maximum depth to which the vertical section of the model could be extended. This procedure allows the number of problem parameters to be reduced. We can also control how the model resolution is modified in the inversion procedure by evaluating it at each iteration. The changes in the resolution are related to the changes in weighting matrices (and therefore, the generalized inverse) during the iterative process. The model resolution is greatly affected by the choice of the parameter N/S.

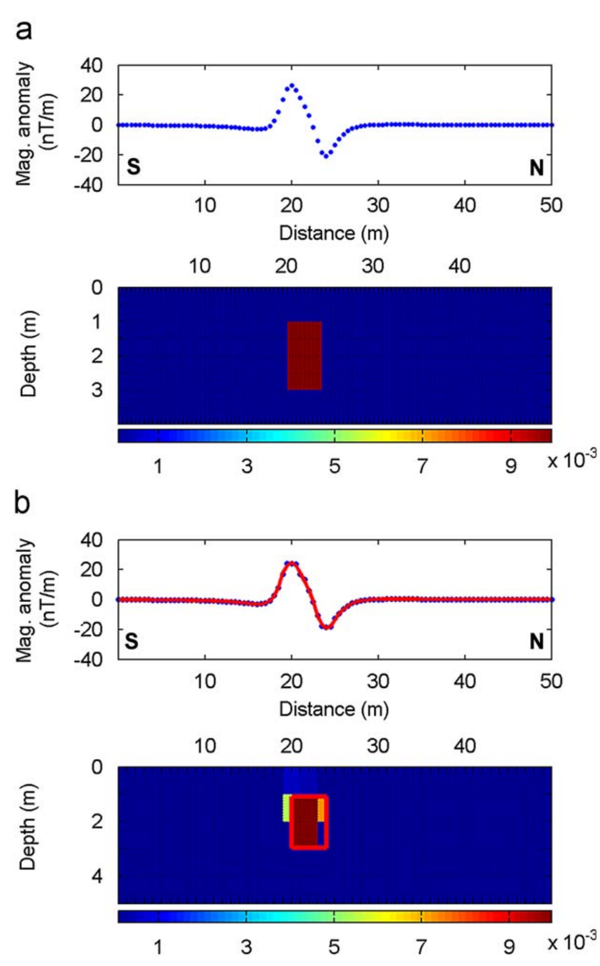

Fig. 5. Inversion result using a different parameterisation with respect to generating model: (a) generating model, 100×8 prisms of $0.5\,m \times 0.5\,m$ size; (b) inversion result, 50×5 prisms of $1\,m \times 1\,m$ size. EMF parameters: $F_e = 46{,}000\,nT$, $I = 60^\circ$, $\beta = 0^\circ$ (profile direction is S–N).

High values mean that the result of the inversion is really compact, even if the fitting with the experimental data is not optimised. This approach is also useful for very noisy data interpretation. On the contrary, with low N/S values, the inversion procedure better fits the data, but the compactness of the solution cannot be obtained.

The choice of the iteration which offers the best fitting is driven by the minimum norm between calculated and experimental data. A quasi-automatic selection of the signal segments that could be considered as carrying information on the targets is proposed ("mask signal"). We drive the inversion operator on those parts of the signal that we call "useful signal", i.e. the main anomalies. The L_2-norm between the calculated and experimental signals is only evaluated in these segments. The "mask signal" approach is based on the following steps (Fig. 3):

- evaluation of the signal power spectrum in the wave number domain (k) using the Fourier transform (Fig. 3b);
- estimation of the k-numbers $k_{-12\,\mathrm{dBh}}$ and $k_{-12\,\mathrm{dBl}}$ which correspond to $-12\,\mathrm{dB}$, i.e. 1/4 of the maximum value of the power spectrum and determination of a band width, in terms of wave length $BW(\lambda)$ (Fig. 3b):

  $BW = 2\pi/k_{-12\,\mathrm{dBl}} - 2\pi/k_{-12\,\mathrm{dBh}}$;
- evaluation of the running signal power γ^2 in dB along the survey line with a running window of size BW consisting of N samples ($N = BW/(\text{sampling interval})$) (Fig. 3c):

  $$\gamma^2 = \frac{1}{N-1}\sum_{i=1}^{N}(y_i)^2,$$

  where N is the number of samples in the running window and y_i the value of the measured signal;
- choice of an energy threshold (in dB) between the "useful signal" and the noise according to the running power level (Fig. 3c);
- determination of the segments, within the magnetic profile, where the main anomalies are located (Fig. 3d).

This operation produces a "mask signal" (Fig. 3d), with as many samples as the profile, which is made by 0's where the signal energy is below and 1's where the signal energy is above the selected energy threshold. In such a way, in the iterative inversion procedure, the L_2-norm between the calculated and experimental signals is evaluated only in the segments obtained multiplying the latter, point to point, by the mask signal. When this method is used, the fitting of what is considered "noise" is strongly reduced and the convergence process is mainly focused on the "useful signal".

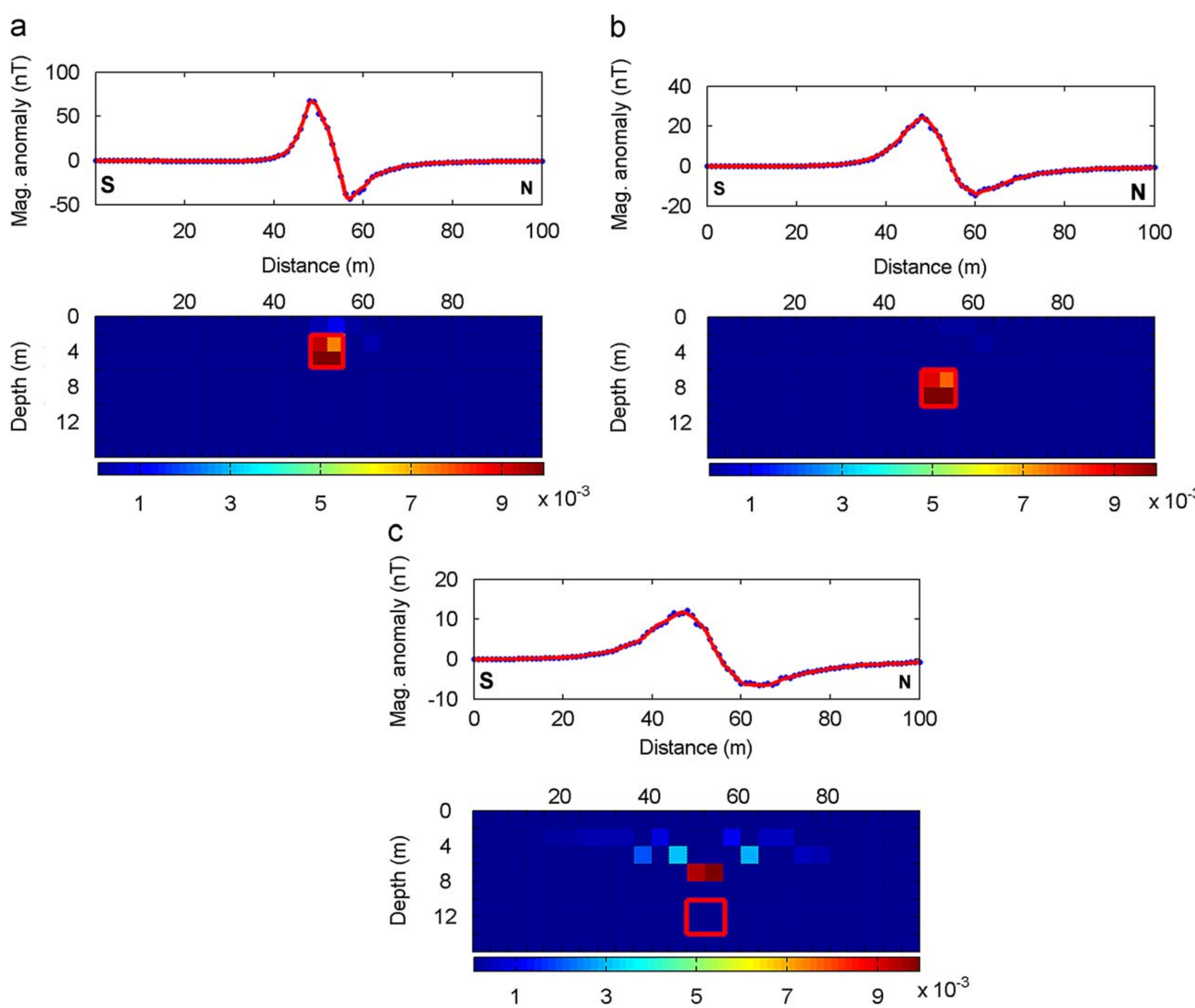

Fig. 6. Inversion results of 3 data sets generated at the same source body sites at different depths. EMF parameters: $F_e = 46{,}000\,\mathrm{nT}$, $I = 60^\circ$ and $\beta = 0^\circ$ (profile direction is S–N).

We suggest adopting the same criterion to determine the value of the N/S parameter to use in the inversion. Therefore, for example, an energy threshold of -18 dB means we keep the signal segments with an energy above 1/8 of the maximum value of the running energy, and the value of N/S would then be 0.125.

Fig. 4 shows the results of an inversion procedure using the "mask signal" (c) and without "mask signal" (b). The synthetic data are perturbed with a normally distributed random noise with a variance of 0.1 nT^2. The problem is underdetermined: the number of observed data (200) is less than the number of prisms of unknown susceptibility (250). The prism dimensions are $2\,\mathrm{m} \times 1\,\mathrm{m}$. We introduce two bodies we refer to as noise (a) into the synthetic example, as well as the source body. The parameterisation is the same for both the modelling and the inversion.

The selection of the parameter N/S influences the noise-weighting matrix (Eq. (6)). It also regularises the generalized inverse in the inversion procedure (Eq. (4)) avoiding round-off problems. These latter are produced by small singular values in the kernel when the generalized inverse is evaluated. We compute the model resolution before the inversion procedure in order to choose the best subsoil gridding with respect to the data; the weighted matrix is not considered in the first iteration. In this case, the singular value decomposition of the kernel permits the rank of the matrix to be evaluated according to a certain tolerance based on the matrix size, the largest singular value and the Matlab floating-point relative accuracy (2^{-52}).

An example with different parameterisation is shown in Fig. 5. In the synthetic model, the dimension of each prism is $0.5\,\mathrm{m} \times 0.5\,\mathrm{m}$, for a total of 100×8 prisms. We evaluated the VGTMF of the source body on a profile of 50 m, with a sampling step of 0.5 m (Fig. 5a). We then perturbed the data with a normally distributed random noise with a variance of 0.05 nT^2. In the inversion procedure, the size of the prisms is $1\,\mathrm{m} \times 1\,\mathrm{m}$, for a total of 50×5 prisms (Fig. 5b).

In order to avoid the tendency of locating the structure too close to the surface (Fig. 6), we introduce a procedure to counteract the natural decay of the kernel and to equalize the possibility of deeper cells being part of the solution with non-zero susceptibility (Li and Oldenburg, 1996). We compute a depth weighting function that, multiplied by the values of the kernel under a measured point, gives a constant value equal to 1:

$$w(z) = (G_{1,j})^{-1/2}, \tag{7}$$

where G is the kernel and j the index of the pixels under the first measured point. This function is absolutely objective and only depends on the kernel. Fig. 7 shows an example of inverting using: (a) the TMF, (b) the VGTMF, (c) the information of the TMF at both

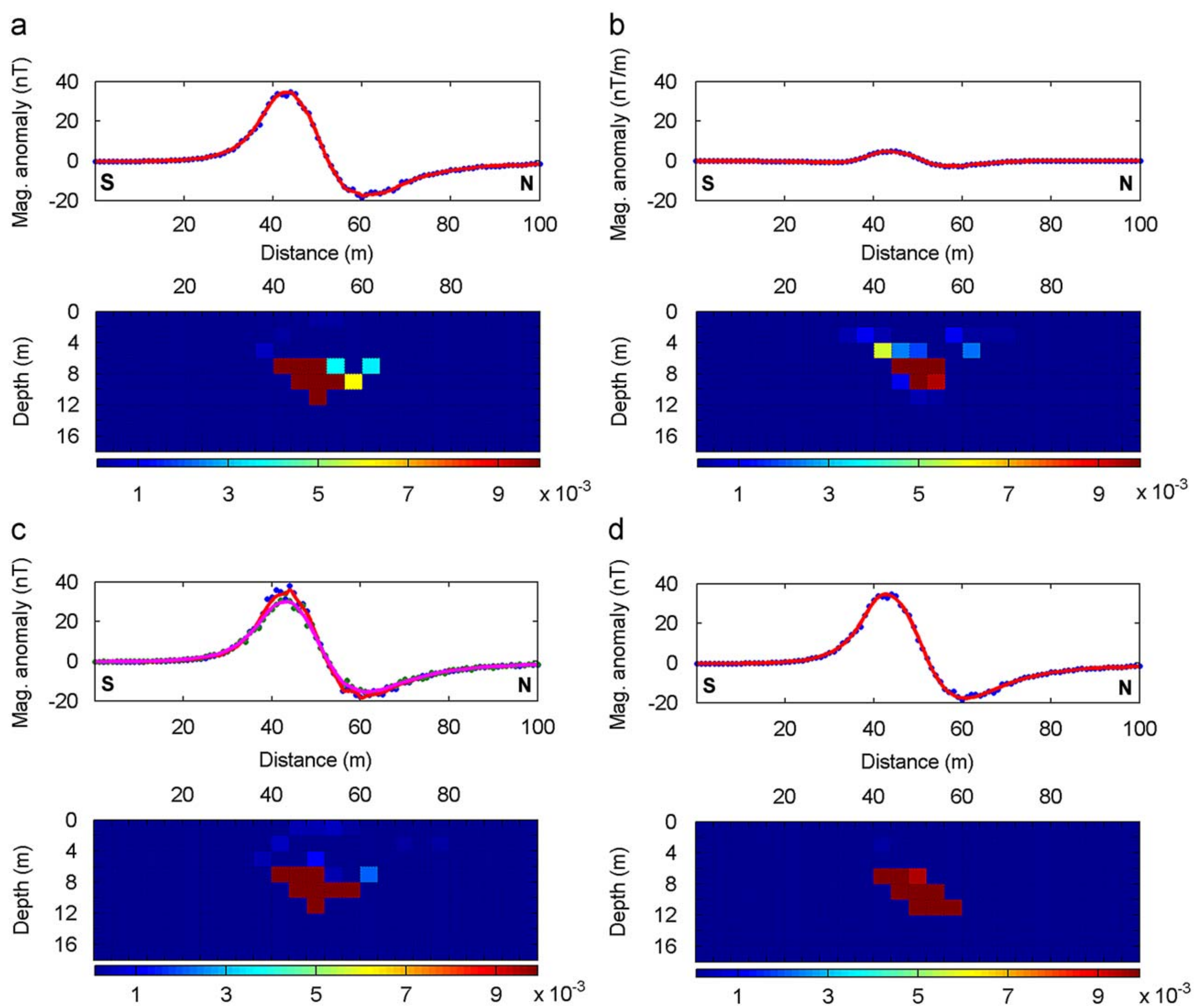

Fig. 7. Inversion results using: (a) the TMF, (b) the VGTMF, (c) information of TMF at both sensors, and (d) depth weighting function. EMF parameters: $F_e = 46{,}000$ nT, $I = 60^\circ$ and $\beta = 0^\circ$ (profile direction is S–N).

sensors, and (d) the depth weighting function. The latter case recovers both the shape and the magnetic susceptibility of the source body. The synthetic data are perturbed with a normally distributed random noise with a variance of 0.1 Tn^2.

3. Results on experimental data

We applied the suggested approach to magnetic data in the well-studied area of the Sabine Necropolis at *Colle del Forno* (700–300 B.C.) at Montelibretti, Rome, in order to compare the inversion results with the evidence obtained in the archaeological excavation. The archaeological site is characterised by *dromos* chamber tombs, most of them unexplored till now. The tombs can be assimilated to cavities of a standard volume of some cubic meters; the entrance to the tombs is a 6 m long corridor with a 1 square meter section. The shallow geology of the area consists of a series of tuffs about 10-m-thick overlying Pleistocene–Quaternary sandy–clayey sediments. A thin layer of topsoil (0.2–0.3 m) covers the tuff.

The magnetic survey was performed along a regular $0.5\,m \times 0.5\,m$ grid using an optical pumped Caesium-vapour magnetometer G858 (Geometrics), in the gradient configuration, on an area which is well known as far as the presence, size and position of the tombs are concerned.

The magnetic susceptibility contrast between the topsoil, subsoil and rocks (topsoil is normally more magnetic than subsoil) makes it possible to detect ditches, pits and other silted-up features that were excavated and then silted or back-filled with topsoil. While back-filled areas produce positive anomalies, less magnetic material introduced into the topsoil, including many kinds of masonry (for example, limestone walls) can produce negative anomalies of the order of some nanoteslas. The same behaviour is related to the presence of cultural voids and tombs whose magnetic anomaly is generated by the lack of magnetic material due to the cavities of the tombs. A diffused magnetisation in the area is mainly due to the presence of topsoil and tuff material and high negative susceptibility contrasts can be expected because of the presence of the tombs. The susceptibility contrast between the topsoil (tuff material) and the void of the chambers and corridor was previously estimated through cross-correlation analysis (Godio and Piro, 2005); according to the previous study, a value of −0.006 S.I. was adopted.

We interpreted two profiles extracted from the vertical gradient map shown in Fig. 8a. The parameters used in the inversion process are:

- prisms along the x-direction = 60;
- prisms along the z-direction = 9;

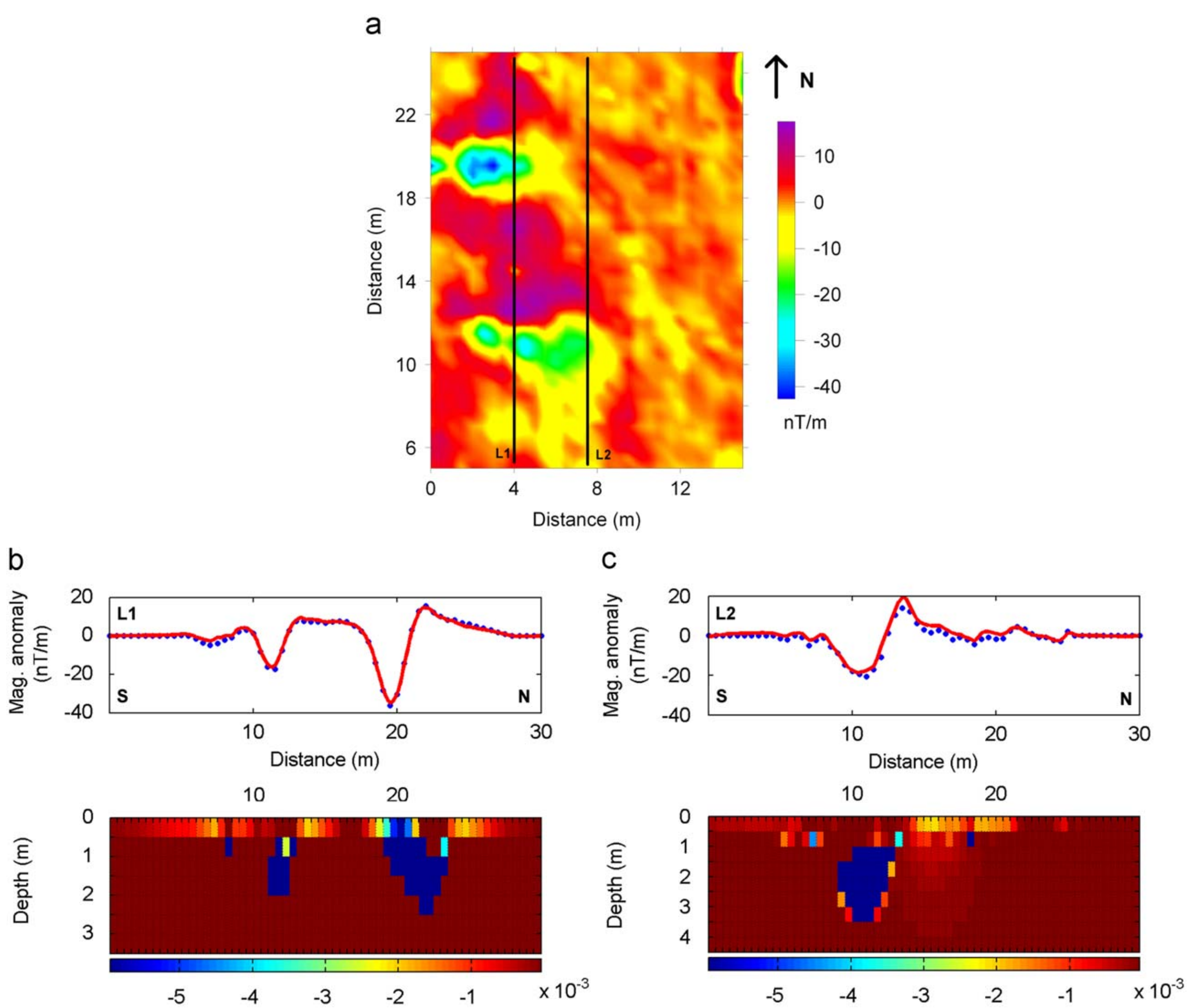

Fig. 8. Sabine necropolis—Colle del Forno (Roma): (a) VGTMF map with trace of profiles selected for subsequent inversion, (b) line 1-inversion result, and (c) line 2-inversion result. EMF parameters: $F_e = 45{,}000\,nT$, $I = 58^\circ$, $\beta = 0^\circ$ (profile direction is S–N).

- prism dimension = 0.5 m × 0.5 m;
- max number of iterations = 10;
- noise/signal = 0.125.

The results are shown in Fig. 8b and c. The spatial position, width and depth of two tombs agree approximately with the results of the excavation. The first profile (Fig. 8b) intercepts the corridor of the first *dromos* (coordinate 11 m) and a second *dromos* at coordinates 19–20 m; the result of the compact magnetic inversion procedure permitted a good match to be obtained between the computed and observed curves. The corridor and *dromos* sections are only slightly overestimated. The second profile (Fig. 8c) intercepts the main *dromos* at the 9 m coordinate.

4. Final remarks

The code, developed in Matlab environment, allows the forward model and the inversion of 2D and $2\frac{1}{2}$D magnetic data of both TMFs, VGTMF and VMF, to be computed. The code is based on some optimisation procedures aimed at improving the solution stability of the inversion and the reliability of the interpretation.

The approach is effective for simple shapes such as prisms and dykes. The simulations performed using synthetic examples of magnetic anomalies generated by compact bodies embedded in an inducing magnetic field show that the code is capable of solving underdetermined problems in the presence of moderate data noise with good accuracy.

The analysis of the model resolution, singular value decomposition and the equalization of the kernel makes it possible to verify the reliability of the interpretation and to control the maximum depth of the data processing. Examples of the application to archaeological data are also given; the code permitted the location and shape of two buried tombs in an ancient necropolis to be defined with good accuracy.

Appendix A. Supporting Information

Supplementary data associated with this article can be found in the online version at: doi:10.1016/j.cageo.2009.04.002.

References

Bhattacharyya, B.K., 1964. Magnetic anomalies due to prism-shaped bodies with arbitrary polarization. Geophysics 29 (4), 517–531.

Cooper, G.R.J., 2006. Interpreting potential field data using continuous wavelet transforms of their horizontal derivatives. Computers & Geosciences 32 (7), 984–992.

Cooper, G.R.J., Cowan, D.R., 2006. Enhancing potential field data using filters based on the local phase. Computers & Geosciences 32 (10), 1585–1591.

Durrheim, R.J., Cooper, G.R.J., 1998. EULDEP: a program for the Euler deconvolution of magnetic and gravity data. Computers & Geosciences 24 (6), 545–550.

Fedi, M., Quarta, T., 1998. Wavelet analysis for the regional-residual and local separation of potential field anomalies. Geophysical Prospecting 46 (5), 507–525.

Fedi, M., Primiceri, R., Quarta, T., Villani, A.V., 2004. Joint application of continuous and discrete wavelet transform on gravity data to identify shallow and deep sources. Geophysical Journal International 156 (1), 7–21.

FitzGerald, D., Reid, A.A., McInerney, P., 2004. New discrimination techniques for Euler deconvolution. Computers & Geosciences 30, 461–469.

Godio, A., Piro, S., 2005. Integrated data processing for archaeological magnetic surveys. The Leading Edge 24, 1138–1144.

Guillen, A., Menichetti, V., 1984. Gravity and magnetic inversion with minimisation of a specific functional. Geophysics 49, 1354–1360.

Last, B.J., Kubik, K., 1983. Compact gravity inversion. Geophysics 48, 713–721.

Li, Y., Oldenburg, D.W., 1996. 3-D inversion of magnetic data. Geophysics 61, 394–408.

Menke, W., 1984. Geophysical Data Analysis: Discrete Inverse Theory. Academic Press Inc., San Diego, California, 285pp.

Moreau, F., Gibert, D., Holschneider, M., Saracco, G., 1997. Wavelet analysis of potential fields. Inverse Problems 13, 165–178.

Narasimha Rao, B., Ramakrishna, P., Markandeyulu, A., 1995. GMINV: a computer program for gravity or magnetic data inversion. Computers & Geosciences 21 (2), 301–319.

Telford, W.M., Gedart, L.P., Sheriff, R.E., 1990. Applied Geophysics. Cambridge University Press, Cambridge, UK, 512pp.

Venkata Raju, D.Ch., 2003. LIMAT: a computer program for least-squares inversion of magnetic anomalies over long tabular bodies. Computers & Geosciences 29 (1), 91–98.